

# High-Pressure Study on the Quenching Mechanism by Oxygen of the Lowest Triplet State in Solution

Masami Okamoto\*

Faculty of Engineering and Design, Kyoto Institute of Technology, Matsugasaki, Sakyo-ku, Kyoto 606-8585, Japan

Fujio Tanaka

College of Integrated Arts and Sciences, Osaka Prefecture University, Gakuen-cho, Sakai 599-8531, Japan

Satoshi Hirayama

Laboratory of Physical Chemistry, Kyoto Institute of Technology, Matsugasaki, Sakyo-ku, Kyoto 606-8585, Japan

Received: July 23, 1998; In Final Form: October 20, 1998

The mechanism for the quenching by oxygen of the lowest triplet state ( $T_1$ ) of 9-acetylanthracene (ACA) in five saturated hydrocarbon solvents at pressures up to 400 MPa was investigated. The quenching rate constants of the  $T_1$  state of ACA,  $k_q^T$ , decrease monotonically with increasing pressure, and the apparent activation volumes for  $k_q^T$  vary in the range 0.8–5.3 cm<sup>3</sup>/mol. It was also found that the plots of  $\ln k_q^T$  against  $\ln \eta$ , where  $\eta$  is solvent viscosity, show significant downward curvatures in all the solvents examined. From measurements by the time-resolved thermal lensing at 0.1 MPa, together with measurements of triplet–triplet absorption spectra as a function of pressure, the yields of the  $T_1$  state of ACA were found to be approximately unity in the experimental conditions examined. The quenching rate constants,  $k_q^S$ , by oxygen of the lowest excited singlet state ( $S_1$ ) of 9,10-dimethylantracene (DMEA) whose van der Waals radius is nearly equal to that of ACA decrease strongly with increasing pressure, and the apparent activation volumes for  $k_q^S$  fall in the range of 9.4–14.9 cm<sup>3</sup>/mol. It was also found that the plots of  $\ln k_q^S$  against  $-\ln \eta$  are linear, with a slope of 0.59–0.71 depending on solvent. These results of  $k_q^S$  are consistent with our previous conclusion that the oxygen quenching of the  $S_1$  state of DMEA is diffusion controlled. The ratio,  $k_q^T/k_q^S$ , is approximately 1/9 in methylcyclohexane but is less than 1/9 in *n*-butane, *n*-pentane, *n*-hexane, and *n*-heptane at 0.1 MPa and 25 °C, and the ratio was found to increase over 1/9 with increasing pressure in all the solvents examined. By the bleaching method of DPBF, coupled with time-resolved luminescence measurements, the yields of singlet oxygen ( $^1\Delta_g$ ) formed by the quenching of the  $T_1$  state of ACA,  $\Phi_\Delta$ , were measured, and the values of  $\Phi_\Delta$  were found to be approximately unity. These results were explained by a kinetic model in which the intersystem crossings between encounter complexes with different spin multiplicities are taken into account. From the analysis based on this model, the pressure dependence of  $k_q^T/k_q^S$  is discussed.

## Introduction

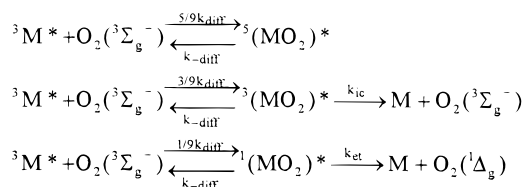
The quenching by oxygen of electronically excited singlet and triplet states of aromatic molecules in solution has been extensively investigated<sup>1,2</sup> and often believed to be diffusion controlled. In fact, the quenching rate constants,  $k_q^S$ , for the lowest excited singlet states ( $S_1$ ) of some aromatic molecules in nonviscous solvents are ca.  $3 \times 10^{10} \text{ M}^{-1} \text{ s}^{-1}$ , which is close to the rate constant for diffusion-controlled reactions evaluated by using the diffusion coefficients of oxygen and aromatic molecules.<sup>3</sup> Recently, we reported the quenching by oxygen of the electronically excited states of a number of mesosubstituted anthracene derivatives as a function of pressure and found that the pressure dependence of  $k_q^S$  as well as its magnitude vary from compound to compound, being dependent on the electronic nature of the substituents.<sup>4</sup> For the anthracene derivatives with one or two electron-donating substituents such as 9,10-dimethylantracene (DMEA), it was concluded that the quenching

of their  $S_1$  states is nearly diffusion controlled judging from the fractional power dependence of  $k_q^S$  on solvent viscosity,  $\eta$ , changed by the application of pressure ( $k_q^S$  is proportional to  $\eta^{-\alpha}$ ), as well as from the magnitude of  $k_q^S$ .<sup>5</sup>

The quenching by oxygen of the lowest triplet states ( $T_1$ ) is not so efficient as compared to that of the  $S_1$  states for most aromatic compounds, and their quenching rate constants,  $k_q^T$ , are on the order of  $10^9 \text{ M}^{-1} \text{ s}^{-1}$  for typical aromatic hydrocarbons.<sup>2</sup> The low quenching ability of the  $T_1$  states has been explained by the mechanism shown in Scheme 1 via the encounter complexes  $^i(\text{MO}_2)^*$  ( $i = 1, 3, \text{ or } 5$ ) that have three different spin multiplicities.<sup>6</sup>

In Scheme 1,  $^i(\text{MO}_2)^*$  ( $i = 1, 3, \text{ or } 5$ ) is formed with  $i/9$  of the diffusion-controlled rate constant,  $k_{\text{diff}}$ , by the requirement of spin statistics. The yield of singlet oxygen ( $\text{O}_2 (^1\Delta_g)$ ),  $S_\Delta$ , by the quenching of  $^3\text{M}^*$  is close to unity for most anthracene derivatives,<sup>7,8</sup> whereas it is less than unity for some ketones<sup>9,10</sup>

## SCHEME 1



and some aromatic hydrocarbons.<sup>11–13</sup> The quenching mechanism shown in Scheme 1 was also supported by measurements of  $S_\Delta$ , although intersystem crossing between encounter complexes is involved for the systems with internal heavy-atom effects<sup>14</sup> and CT interactions.<sup>15,16</sup>

We observed that  $k_q^T/k_q^S$  is 0.13, close to 1/9 for both anthracene and 9-methylanthracene at 0.1 MPa in methylcyclohexane, in which  $k_q^S$  is concluded to be nearly diffusion controlled, but it increases monotonically with increasing pressure and was found to be 0.33 and 0.32 at 400 MPa for anthracene and 9-methylanthracene, respectively.<sup>4,5</sup> According to Scheme 1, when the quenching is fully diffusion controlled, we have a relation that  $k_q^T = k_{diff}/9$  if  $S_\Delta = 1$ , or  $k_q^T = 4k_{diff}/9$  if  $S_\Delta = 0.25$ . This implies that the increased participation of  $k_{ic}$  will lower  $S_\Delta$  by pressure, but unfortunately, the pressure dependence of  $S_\Delta$  is not measured. Furthermore, the fact that a plot of  $\ln k_q^T$  against  $\ln \eta$  shows significant downward curvatures<sup>4,5</sup> suggests the existence of processes competitive with diffusion as well as the contribution of a spin statistical factor. Thus, the quenching mechanism by oxygen of the  $T_1$  states is not yet fully understood.

The present study is focused on the quenching mechanism by oxygen of the  $T_1$  state of 9-acetylanthracene (ACA) from measurements of  $k_q^T$  and the yield of the  $T_1$  state, together with measurements of the yield of singlet oxygen formed by the quenching as a function of pressure up to 400 MPa. ACA was used since this molecule does not fluoresce in solution at room temperature and the pressures up to 400 MPa, although it fluoresces significantly at very high pressure, above about 4 GPa.<sup>17</sup> The rate constant for diffusion between ACA and oxygen,  $k_{diff}$ , which is needed to discuss the quenching mechanism of the triplet-state, is expected to be reduced significantly by the application of high pressure. For comparison, we also measured the quenching constant by oxygen of the fluorescence of 9,10-dimethylanthracene (DMEA) whose van der Waals radius (0.365 nm) is close to that of ACA (0.356 nm)<sup>18</sup> and assumed that the diffusion coefficients are the same. Furthermore, to investigate the relationship between  $k_q^S$  and  $k_q^T$ , these measurements of the  $S_1$  and  $T_1$  states were carried out as a function of pressure in five saturated hydrocarbons including methylcyclohexane, for which the pressure dependence of  $k_q^T$  and  $k_q^S$  was reported previously.<sup>4,5</sup>

### Experimental Section

9-Acetylanthracene (ACA) (Aldrich Chemical Co.) was chromatographed twice on silica gel and developed and eluted with *n*-pentane, followed by recrystallization from ethanol twice. 9,10-Dimethylanthracene (DMEA) (Aldrich Chemical Co.) was recrystallized from methanol and then purified by thin-layer chromatography. Diphenylisobenzofuran (DPBF) (Aldrich Chemical Co.) was used without further purification. *n*-Butane (Tokyo Kasei Kogyo Co., Ltd.), of guaranteed grade, and *n*-pentane (Merck), *n*-hexane (Merck), *n*-heptane (Dojin Pure Chemicals Co.), and methylcyclohexane (MCH, Dojin Pure Chemicals Co.) of spectroscopic grade were used as received.

Transient absorption measurements at high pressure were performed by using an 8 ns pulse from a nitrogen laser (337.1 nm) for excitation and a xenon analyzing flash lamp positioned at right angles to the direction of the excitation pulse. The analyzing light intensities were monitored by a Hamamatsu R928 photomultiplier through a Ritsu MC-25N monochromator, and the signal was digitized by using a Hewlett-Packard 54510A digitizing oscilloscope. Fluorescence decay curve measurements at high pressure were performed by using a 0.3 ns pulse from a PRA LN103 nitrogen laser for excitation. The fluorescence intensities were measured by a Hamamatsu R1635-02 photomultiplier through a Ritsu MC-25NP monochromator, and the resulting signal was digitized by using a LeCroy 9362 digitizing oscilloscope. All data were analyzed by using a NEC 9801 microcomputer, which was interfaced to the digitizers. The details about the associated high-pressure techniques have been described elsewhere.<sup>19,20</sup>

The concentration of ACA for the triplet lifetime measurements was adjusted to be ca. 0.8 in absorbance (1 cm cell) at 337.1 nm, and that of DMEA for the fluorescence lifetime measurements was less than 0.1 at maximum absorption wavelength in order to minimize the reabsorption effects. In the measurements of  $T-T'$  absorption spectra as a function of pressure, the higher concentration of ACA (ca. 1.6) was chosen in order to minimize the concentration dependence on the number of absorbed photons. The sample solutions of *n*-hexane, *n*-heptane, and MCH were deoxygenated by bubbling nitrogen gas under nitrogen atmosphere, and the concentrations of dissolved oxygen in those solvents were determined from the solubility data of oxygen.<sup>4,21,22</sup> The increase in the concentration of oxygen by applying high pressure was corrected by using the compressibility of the solvent.<sup>23–32</sup>

Since *n*-butane and *n*-pentane are a gas and a very volatile liquid under the normal condition, respectively, the quenching experiments in such solvents were carried out with a different procedure. An appropriate volume of a hexane stock solution of ACA or DMEA was placed into a high-pressure cell with four optical sapphire windows. The solvent was evaporated, and then the high-pressure cell was evacuated and filled with deoxygenated solvent from a high-pressure syringe pump (500 MPa). The oxygen concentration was determined by introducing a known pressure of synthesized air (oxygen/nitrogen/argon = 21/78/1 vol %, Taiyo Oxygen Co.) into the high-pressure cell. Complete dissolution of oxygen into the solvent at 25 °C was checked by measuring the triplet lifetime of ACA or the fluorescence lifetime of DMEA as a function of time.

The phosphorescence decay curves of singlet oxygen at 1270 nm were measured as a function of pressure by a similar method described previously.<sup>33</sup> In the present work, the element used in the near-IR detection system was replaced by an InGaAs sensor (1 mm  $\phi$ , Hamamatsu G5832–01), which was biased reversely at 5 V since the time response is much better (the total rise time was about 0.4  $\mu$ s). The bleaching of DPBF by singlet oxygen was determined as described previously.<sup>34,35</sup> The concentrations of ACA were adjusted to give ca. 0.5 and 1.6 in absorbance at 337.1 nm (1 cm cell) for the phosphorescence and bleaching measurements, respectively.

The absorption spectra as a function of pressure were recorded on a Shimadzu UV 260 equipped with the high-pressure optical cell. The spectra of the sample solution and the solvent were taken separately, and the corrected spectra were obtained by subtracting the latter from the former spectra.

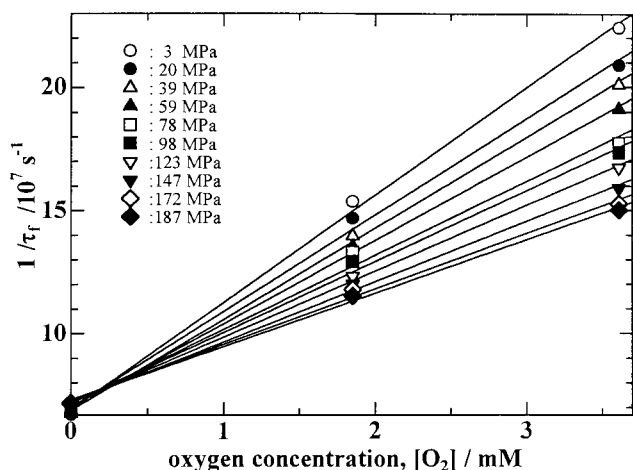


Figure 1. Plots of  $1/\tau_f$  for DMEA against the concentration of oxygen,  $[O_2]$ , in *n*-butane at 10 different pressures.

TABLE 1: Oxygen-Quenching Rate Constants for the  $S_1$  State of DMEA,  $k_q^S$ , and the  $T_1$  State of ACA,  $k_q^T$ , in *n*-Butane

$P$ (MPa)	$\eta$ (cP)	DMEA, $k_q^S$ ( $10^{10} \text{ M}^{-1} \text{ s}^{-1}$ )	ACA <sup>a</sup> , $k_q^T$ ( $10^9 \text{ M}^{-1} \text{ s}^{-1}$ )
3	0.160	$4.35 \pm 0.16$	3.31
20	0.198	$3.92 \pm 0.17$	3.40
39	0.230	$3.70 \pm 0.10$	3.39
59	0.272	$3.38 \pm 0.09$	3.29
78	0.309	$3.00 \pm 0.22$	3.24
98	0.348	$2.87 \pm 0.16$	3.16
123	0.397	$2.69 \pm 0.06$	2.97
147	0.446	$2.45 \pm 0.10$	2.88
172	0.498	$2.26 \pm 0.12$	2.82
187	0.530	$2.16 \pm 0.08$	2.74

<sup>a</sup> Within  $\pm 5\%$ .

Temperature was controlled at  $25 \pm 0.2$  °C. Pressure was measured by a calibrated manganin wire or a Minebea STD-5000K strain gauge.

## Results

The quenching by oxygen of the  $T_1$  state of ACA involves, undoubtedly, the diffusion processes. Therefore, first, we describe the fluorescence quenching by oxygen of DMEA, which gives the diffusion-controlled rate constant, and then the results of the  $T_1$  state of ACA are presented.

**Fluorescence Quenching of DMEA.** Fluorescence decay curves were analyzed satisfactorily by a single-exponential function in all the conditions examined. The quenching rate constant for the  $S_1$  state of DMEA,  $k_q^S$ , was determined by eq 1 if the concentration of dissolved oxygen is known

$$1/\tau_f - 1/\tau_f^0 = k_q^S [O_2] \quad (1)$$

where  $\tau$  and  $\tau_f^0$  represent the fluorescence lifetimes in the aerated and deaerated solutions, respectively. Typical examples of the plots of  $1/\tau_f$  against the concentration of oxygen in *n*-butane are shown in Figure 1. The values of  $k_q^S$  were determined from the slopes of the least-squares plots. The results obtained are listed in Tables 1–5 together with the data on solvent viscosity,  $\eta$ .<sup>23–32</sup>

As seen in Tables 1–5,  $k_q^S$  decreases significantly with increasing pressure in solvents studied in this work. The pressure

TABLE 2: Oxygen-Quenching Rate Constants for the  $S_1$  State of DMEA,  $k_q^S$ , and the  $T_1$  State of ACA,  $k_q^T$ , and the Values of  $\Phi_{\Delta}(P)/\Phi_{\Delta}(0)$  in *n*-Pentane

$P$ (MPa)	$\eta$ (cP)	DMEA, $k_q^S$ ( $10^{10} \text{ M}^{-1} \text{ s}^{-1}$ )	ACA <sup>a</sup> , $k_q^T$ ( $10^9 \text{ M}^{-1} \text{ s}^{-1}$ )	$\Phi_{\Delta}(P)/\Phi_{\Delta}(0)$
0.1	0.229	$4.08 \pm 0.20$	3.19	$1.0 \pm 0.1$
50	0.350	$3.36 \pm 0.12$	2.99	$1.0 \pm 0.1$
100	0.484	$2.78 \pm 0.12$	2.86	$1.0 \pm 0.1$
150	0.629	$2.36 \pm 0.10$	2.68	$1.1 \pm 0.1$
200	0.786	$2.01 \pm 0.10$	2.52	$1.0 \pm 0.1$
250	1.002	$1.77 \pm 0.14$	2.39	$1.1 \pm 0.1$
300	1.202	$1.49 \pm 0.03$	2.24	$1.0 \pm 0.1$
350	1.443	$1.29 \pm 0.05$	2.13	$1.1 \pm 0.1$
400	1.726	$1.14 \pm 0.05$	2.02	$1.1 \pm 0.1$

<sup>a</sup> Within  $\pm 3\%$ .

TABLE 3: Oxygen-Quenching Rate Constants for the  $S_1$  State of DMEA,  $k_q^S$ , and the  $T_1$  State of ACA,  $k_q^T$ , and the Values of  $\Phi_{\Delta}(P)/\Phi_{\Delta}(0)$  in *n*-Hexane

$P$ (MPa)	$\eta$ (cP)	DMEA, $k_q^S$ ( $10^{10} \text{ M}^{-1} \text{ s}^{-1}$ )	ACA <sup>a</sup>		$\Phi_{\Delta}(P)/\Phi_{\Delta}(0)$
			$\tau_T^b$ (ns)	$k_q^T$ ( $10^9$ ) $\text{M}^{-1} \text{ s}^{-1}$	
0.1	0.294	$3.52 \pm 0.13$	99.5	3.25	$1.0 \pm 0.1$
50	0.472	$2.78 \pm 0.11$	100.6	3.03	$1.0 \pm 0.1$
100	0.650	$2.26 \pm 0.10$	101.6	2.89	$1.0 \pm 0.1$
150	0.849	$1.87 \pm 0.09$	107.8	2.65	$1.0 \pm 0.1$
200	1.063	$1.56 \pm 0.09$	109.6	2.54	$1.1 \pm 0.1$
250	1.310	$1.33 \pm 0.08$	116.1	2.36	$1.0 \pm 0.1$
300	1.610	$1.13 \pm 0.08$	126.3	2.13	$1.0 \pm 0.1$
350	1.948	$0.98 \pm 0.07$	128.2	2.07	$1.1 \pm 0.1$
400	2.368	$0.84 \pm 0.07$	141.9	1.84	$1.0 \pm 0.1$

<sup>a</sup> Within  $\pm 3\%$ . <sup>b</sup> Lifetimes of the  $T_1$  state of ACA in air-saturated *n*-hexane (3.09 mM at 0.1 MPa).

TABLE 4: Oxygen Quenching Rate Constants for the  $S_1$  State of DMEA,  $k_q^S$ , and the  $T_1$  State of ACA,  $k_q^T$ , and the Values of  $\Phi_{\Delta}(P)/\Phi_{\Delta}(0)$  in *n*-Heptane.

$P$ (MPa)	$\eta$ (cP)	DMEA, $k_q^S$ ( $10^{10} \text{ M}^{-1} \text{ s}^{-1}$ )	ACA <sup>a</sup>		$\Phi_{\Delta}(P)/\Phi_{\Delta}(0)$
			$\tau_T^b$ (ns)	$k_q^T$ ( $10^9$ ) $\text{M}^{-1} \text{ s}^{-1}$	
0.1	0.382	$3.21 \pm 0.06$	110.8	2.93	$1.0 \pm 0.1$
50	0.587	$2.40 \pm 0.07$	113.0	2.71	$1.0 \pm 0.1$
100	0.857	$1.91 \pm 0.11$	119.7	2.47	$1.1 \pm 0.1$
150	1.209	$1.61 \pm 0.10$	125.5	2.28	$1.1 \pm 0.1$
200	1.652	$1.25 \pm 0.04$	134.3	2.09	$1.1 \pm 0.1$
250	2.192	$1.05 \pm 0.06$	141.3	1.95	$1.1 \pm 0.1$
300	2.835	$0.93 \pm 0.03$	152.5	1.78	$1.1 \pm 0.1$
350	3.582	$0.77 \pm 0.06$	164.1	1.63	$1.1 \pm 0.1$
400	4.437	$0.66 \pm 0.08$	177.1	1.49	$1.0 \pm 0.1$

<sup>a</sup> Within  $\pm 3\%$ . <sup>b</sup> Lifetimes of the  $T_1$  state of ACA in air-saturated *n*-heptane (3.08 mM at 0.1 MPa).

dependence of  $k_q^S$  is shown in Figure 2a. The apparent activation volumes for  $k_q^S$ ,  $\Delta V_q^{S\ddagger}$ , evaluated by eq 2 ( $i = S$ ) are listed in Table 6 together with those of the solvent viscosity. As seen in

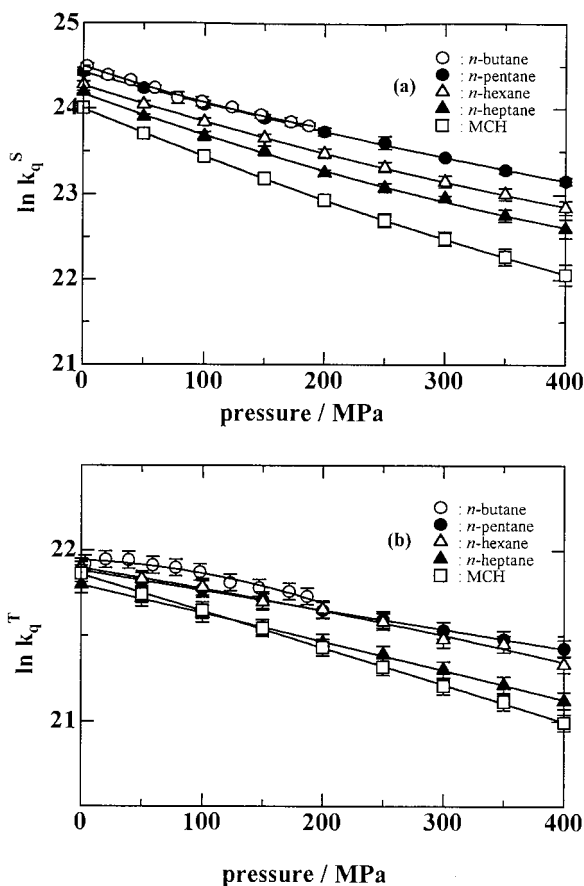
$$RT(\partial \ln k_q^i / \partial P)_T = -\Delta V_q^{i\ddagger} \quad (2)$$

Table 6, the values of  $\Delta V_q^{S\ddagger}$  are of the magnitude of 10–14  $\text{cm}^3/\text{mol}$ , which lies in the range of positive activation volumes found for the nearly diffusion-controlled fluorescence quenching by oxygen of anthracene derivatives that have one or two electron-donating substituents.<sup>4</sup> The apparent activation volume for solvent viscosity,  $\Delta V_{\eta}^{\ddagger}$ , was calculated to be in the range 22–24  $\text{cm}^3/\text{mol}$  using data of solvent viscosity,  $\eta$ .<sup>23–32</sup> The large difference between  $\Delta V_q^{S\ddagger}$  and  $\Delta V_{\eta}^{\ddagger}$  may be interpreted by the fact that the fluorescence quenching with a nearly diffusion-controlled rate shows the fractional power dependence of  $\eta$  on

**TABLE 5: Oxygen-Quenching Rate Constants for the S<sub>1</sub> State of DMEA,  $k_q^S$ , and the T<sub>1</sub> State of ACA,  $k_q^T$ , and the Values of  $\Phi_{\Delta}(P)/\Phi_{\Delta}(0)$  in MCH**

<i>P</i> (MPa)	$\eta$ (cP)	DMEA <sup>a</sup> , $k_q^S$ (10 <sup>10</sup> M <sup>-1</sup> s <sup>-1</sup> )	ACA <sup>b</sup>		$\Phi_{\Delta}(P)/\Phi_{\Delta}(0)$
			$\tau_T^c$ (ns)	$k_q^T$ (10 <sup>9</sup> M <sup>-1</sup> s <sup>-1</sup> )	
0.1	0.674	2.66 ± 0.09	127.6	3.13	1.0 ± 0.1
50	1.143	1.97 ± 0.08	138.1	2.77	1.1 ± 0.1
100	1.739	1.51 ± 0.07	147.0	2.52	1.0 ± 0.1
150	2.542	1.17 ± 0.06	159.8	2.27	1.0 ± 0.1
200	3.752	0.91 ± 0.06	175.2	2.03	1.0 ± 0.1
250	5.146	0.72 ± 0.06	192.6	1.81	1.1 ± 0.1
300	7.211	0.58 ± 0.05	212.9	1.62	1.0 ± 0.1
350	10.02	0.47 ± 0.05	230.4	1.48	
400	12.81	0.38 ± 0.05	254.8	1.31	1.0 ± 0.1

<sup>a</sup> Reference 36. <sup>b</sup> Reference 4. <sup>c</sup> Lifetimes of the T<sub>1</sub> state of ACA in air-saturated MCH (2.5 mM at 0.1 MPa).



**Figure 2.** Plots of  $\ln k_q^S$  against pressure (a) and plots of  $\ln k_q^T$  against pressure (b) in five solvents. Solid lines were drawn by assuming that  $\ln k_q^i = A + BP + CP^2$  ( $i = S$  or  $T$ ).

$k_q^S$  ( $k_q^S$  is proportional to  $\eta^{-\alpha}$ ) as reported previously.<sup>4,5</sup> In fact, the plots of  $\ln k_q^S$  against  $-\ln \eta$  are almost linear in the solvents examined, and the values of  $\alpha$  determined by the least-squares plots are  $0.59 \pm 0.02$ ,  $0.64 \pm 0.02$ ,  $0.71 \pm 0.02$ ,  $0.64 \pm 0.01$ , and  $0.64 \pm 0.01$ <sup>5</sup> in *n*-butane, *n*-pentane, *n*-hexane, *n*-heptane, and MCH, respectively; they are comparable with those for the anthracene derivatives where fluorescence is quenched nearly collisionally. In variable temperature measurements for the fluorescence quenching by oxygen of chrysene at 0.1 MPa,<sup>37</sup> a linear relation between  $\ln(k_q^S/T)$  and  $-\ln \eta$  was found ( $\beta = 0.70$  in toluene) and the quenching was concluded to be diffusion controlled. Thus, it may be concluded that the fluorescence quenching under consideration is fully or nearly diffusion controlled.

**TABLE 6: Apparent Activation Volumes<sup>a</sup> (cm<sup>3</sup>/mol) for the Quenching Rate Constants by Oxygen for the S<sub>1</sub> State of DMEA,  $\Delta V_q^S$ , and T<sub>1</sub> State of ACA,  $\Delta V_q^T$ , and the Values of  $k_{\text{bim}}$  and  $\gamma$** 

solvent	$\Delta V_q^{S\ddagger}$	$\Delta V_q^{T\ddagger}$	$k_{\text{bim}}^b$ (10 <sup>10</sup> M <sup>-1</sup> s <sup>-1</sup> )	$\gamma^b$ (10 <sup>10</sup> M <sup>-1</sup> s <sup>-1</sup> )
<i>n</i> -butane	12.1 ± 0.7	0.8 ± 0.7 (3.0 ± 0.3)	4.8 ± 0.5	0.20 ± 0.03
<i>n</i> -pentane	9.4 ± 0.2	3.0 ± 0.2	4.9 ± 0.1	0.16 ± 0.01
<i>n</i> -hexane	11.1 ± 0.2	2.8 ± 0.3	5.5 ± 0.4	0.18 ± 0.01
<i>n</i> -heptane	12.7 ± 0.5	4.0 ± 0.2	5.5 ± 0.4	0.14 ± 0.01
MCH	14.0 ± 0.2	5.4 ± 0.1	7.1 ± 0.5	0.17 ± 0.01

<sup>a</sup> Apparent activation volumes were calculated according to the equation,  $RT(\partial \ln k_q^i/\partial P)_T = -\Delta V_q^{i\ddagger}$  ( $i = S$  or  $T$ ) by assuming that  $\ln k_q^i = A + BP + CP^2$  or  $\ln k_q^T = A' + B'P$  (value in parentheses). <sup>b</sup> The mean values in the five solvents are  $(5.4 \pm 0.3) \times 10^{10}$  and  $(0.17 \pm 0.01) \times 10^{10}$  M<sup>-1</sup> s<sup>-1</sup> for  $k_{\text{bim}}$  and  $\gamma$ , respectively.

In the discussion of the quenching mechanism by oxygen of the T<sub>1</sub> state of ACA described below, we assume that the rate constant for diffusion,  $k_{\text{diff}}$ , for ACA is equal to  $k_q^S$  for DMEA.

**Quenching Rate Constants for the T<sub>1</sub> State of ACA.** The decay curves of the T–T' absorption were described satisfactorily by a single-exponential function in all the conditions examined. The quenching rate constant for the T<sub>1</sub> state,  $k_q^T$ , was determined by

$$1/\tau_T - 1/\tau_T^0 = k_q^T[\text{O}_2] \quad (3)$$

where  $\tau_T$  and  $\tau_T^0$  are the triplet-state lifetimes of ACA in the aerated and deaerated solutions, respectively. In the determination of  $k_q^T$ , the term  $1/\tau_T^0$  was neglected since  $\tau_T^0$  is significantly longer than  $\tau_T$ . The values of  $\tau_T$  in *n*-hexane, *n*-heptane, and MCH are also listed in Tables 3, 4, and 5, respectively, and those of  $k_q^T$  in five solvents are listed in Tables 1–5.

As seen in Tables 1–5,  $k_q^T$  decreases with increasing pressure in the solvents studied, but its pressure dependence is much smaller than that of  $k_q^S$ . The pressure dependence of  $k_q^T$  is shown in Figure 2b. The apparent activation volumes for  $k_q^T$ ,  $\Delta V_q^{T\ddagger}$ , evaluated by eq 2 ( $i = T$ ) are listed in Table 6. It can be seen from Table 6 that the magnitude of  $\Delta V_q^{T\ddagger}$  is nearly equal to that for other anthracene derivatives.<sup>4</sup> The plots of  $\ln k_q^T$  against  $\ln \eta$ , which were linear for the nearly collisional fluorescence quenching as mentioned in the previous section, showed significant downward curvatures in the solvents examined. For example, the slopes decreased monotonically from  $-0.12$  at 0.1 MPa to  $-0.34$  at 400 MPa in *n*-pentane. These observations are common to the quenching by oxygen of the T<sub>1</sub> states of the anthracene derivatives.<sup>4, 5</sup>

**Pressure Dependence of Triplet Quantum Yield.** Figure 3 shows the pressure dependence of the T–T' absorption spectra of ACA in *n*-pentane. As seen in Figure 3, the spectra show a gradual red shift, but the maximum absorbance does not change with increasing pressure. This suggests that the quantum yield for the formation of the triplet state of ACA,  $\Phi_T$ , is approximately independent of pressure provided that the pressure dependence of the molar extinction coefficient is not significant. Such a pressure dependence of the T–T' absorption spectra of ACA was observed in *n*-hexane, *n*-heptane, and MCH as well.

ACA does not fluoresce in solution at room temperature and 0.1 MPa, and this has been ascribed to a very fast intersystem crossing process ( $\Phi_T = 1$ ).<sup>38, 39</sup> We measured the triplet state quantum yield at 0.1 MPa by time-resolved thermal lensing and found that the values of  $\Phi_T$  are practically unity in nonpolar solvents such as *n*-hexane (0.97), MCH (1.0), and benzene



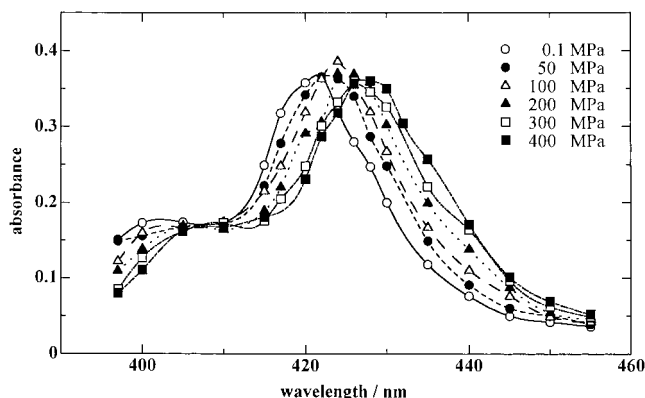
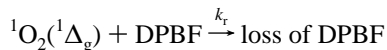


**Figure 3.** Transient absorption spectra of ACA in *n*-pentane observed at 100 ns after the laser pulse excitation at five different pressures.

(0.96).<sup>40</sup> Combining these results with the pressure-insensitive intensity of the T–T' absorption, it may be concluded that  $\Phi_T$  is unity at pressures up to 400 MPa in the four solvents examined in this work. This conclusion may be also valid for the ACA/*n*-butane system, although we did not measure the T–T' absorption spectra in this solvent as a function of pressure.

**Pressure Dependence of the Quantum Yield of Singlet Oxygen.** Singlet oxygen ( $^1\text{O}_2(^1\Delta_g)$ ) generated by the oxygen quenching of electronically excited states in the presence of DPBF decays as follows:



According to this scheme, the absorbance of DPBF (410 nm) at a time  $t$ ,  $A(t)$ , is given by

$$A(t) = A(\infty) + \{A(0) - A(\infty)\} \exp(-k_{\text{obs}}t) \quad (4)$$

where

$$k_{\text{obs}} = k_\Delta + k_T[\text{DPBF}]$$

and  $A(0)$  and  $A(\infty)$  are the absorbances at  $t = 0$  and  $t = \infty$ , respectively.<sup>33,34</sup> The time course of the bleaching reaction was analyzed satisfactorily by curve-fitting to eq 4 using the iterative nonlinear least-squares method, and the values of  $A(0) - A(\infty)$  and  $k_{\text{obs}}$  were determined in *n*-pentane, *n*-hexane, *n*-heptane, and MCH.

Since  $\Phi_T$  is unity for the experimental conditions examined in this work, the ratio of the quantum yield for the formation of singlet oxygen at  $P$  to that at 0.1 MPa,  $\Phi_\Delta(P)/\Phi_\Delta(0.1)$ , is given by

$$\frac{\Phi_\Delta(P)}{\Phi_\Delta(0.1)} = \left( \frac{\tau_\Delta}{\tau_\Delta - \tau_{\text{obs},P}} \right) \left( \frac{\tau_\Delta - \tau_{\text{obs}}}{\tau_\Delta} \right) \left( \frac{\epsilon_{0.1}}{\epsilon_P} \right) \frac{\{A(0) - A(\infty)\}_P}{\{A(0) - A(\infty)\}_{0.1}} \quad (5)$$

where  $\tau_{\text{obs}} = 1/k_{\text{obs}}$  and  $\epsilon$  and  $\tau_\Delta (=1/k_\Delta)$  represent the molar extinction coefficient of DPBF at 410 nm and the lifetime of singlet oxygen in the absence of DPBF, respectively. The correction for  $\epsilon_{0.1}/\epsilon_P$  was relatively small, 1.04 in *n*-pentane (410 nm), 1.02 in *n*-hexane (412 nm), 1.05 in *n*-heptane (412 nm), and 1.03 in MCH (410 nm) on going from 0.1 to 400 MPa at 25 °C. The values of  $\tau_\Delta$  determined by the phosphorescence decay measurements of singlet oxygen in the four solvents

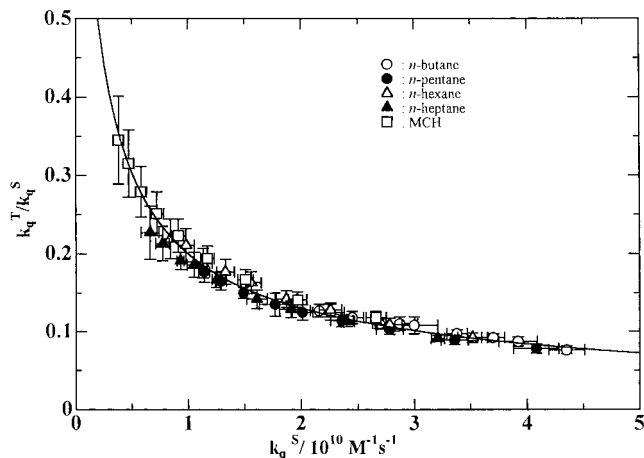


**Figure 4.** Plots of  $k_q^T/k_q^S$  against  $k_q^S$  in five solvents at 25 °C.

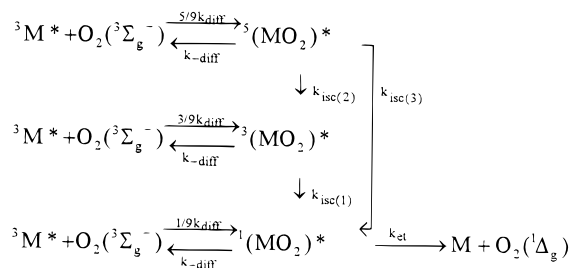
except for *n*-butane decreased significantly with increasing pressure; for example,  $\tau_\Delta$  decreased from 34.3 to 13.4  $\mu\text{s}$  on going from 0.1 to 400 MPa in *n*-pentane. Such a pressure dependence of the lifetime may be explained in the framework of the works reported by us<sup>33,34</sup> and others,<sup>41</sup> and hence, no further discussion is made here. By using the values of  $\tau_\Delta$ , together with the values determined by the bleaching method, we calculated the values of  $\Phi_\Delta(P)/\Phi_\Delta(0.1)$  from eq 5. The results are summarized in Tables 2–5. It can be seen in Tables 2–5 that the quantum yield for the formation of singlet oxygen is independent of pressure in the solvents examined in this work.

The  $\Phi_\Delta(0.1)$  values in the four solvents except for *n*-butane were evaluated by comparing them with the results of the bleaching experiments sensitized by *p*-methoxyacetophenone containing naphthalene in cyclohexane where  $\Phi_\Delta(0.1) = 1.0$ .<sup>42</sup> Phosphorescence decay measurements in this reference sensitizer system give  $22.6 \pm 0.1 \mu\text{s}$  for the lifetime of singlet oxygen,  $\tau_\Delta$ . For the system ACA/cyclohexane we find  $\tau_\Delta = 22.9 \pm 0.1 \mu\text{s}$ . The lifetimes obtained are in good agreement with the values reported by other groups. The difference in  $\epsilon$  at 410 nm between cyclohexane and the solvents examined was very small, and hence the correction for  $\epsilon$  was neglected in eq 5. Using these results, together with the values of  $\tau_\Delta$  at 0.1 MPa, the values of  $\Phi_\Delta(0.1)$  for ACA as a sensitizer were found to be approximately unity in *n*-pentane, *n*-hexane, *n*-heptane, and MCH. The  $\Phi_\Delta(0.1)$  values were also evaluated by comparing the value of the phosphorescence intensity extrapolated to time = 0 for ACA/solvent with that for the reference sensitizer/solvent and were found to be approximately unity in the four solvents.

## Discussion

In the present work, we observed the quantum yields of the  $T_1$  state of ACA are unity and also those for the singlet oxygen formation are unity in the solvents examined at pressures up to 400 MPa at 25 °C. These findings suggest that the rate constant  $k_{ic}$  for the decay process from the encounter complex with the spin multiplicity of triplet is negligibly small. Figure 4 shows plots of  $k_q^T/k_q^S$  against  $k_q^S$ . Since  $k_q^S$  is reasonably assumed to be a diffusion-controlled rate constant, the ratio,  $k_q^T/k_q^S$ , is equal to 1/9, as evaluated by spin statistics, if the quenching of the  $T_1$  state is diffusion controlled. However, it can be seen in Figure 4 that the ratio,  $k_q^T/k_q^S$ , increases with decreasing  $k_q^S$ ; for example, it increases from 0.075 (3 MPa) to 0.13 (187 MPa) in butane and from 0.12 (0.1 MPa) to 0.34 (400 MPa) in MCH. In previous works,<sup>4,5</sup> we measured both  $k_q^T$  and  $k_q^S$  for the anthracene derivatives as a function of pressure, and found

## SCHEME 2



similar pressure dependence of  $k_q^T/k_q^S$ , although the values of  $S_\Delta$  were not measured. In the present system, the step of  $k_{\text{ic}}$  in Scheme 1 can be neglected since the quantum yields for singlet oxygen formation are unity. Therefore, the fact that  $k_q^T/k_q^S$  increases with increasing pressure indicates a participation of the intersystem crossing between the encounter complexes that is increased by pressure. Hence, the quenching mechanism should be modified as shown in Scheme 2 in which the steps of  $k_{\text{isc}(1)}$ ,  $k_{\text{isc}(2)}$ , and  $k_{\text{isc}(3)}$  are taken into account. Similar quenching mechanisms involving the intersystem crossing between the encounter complexes have been proposed for the systems with CT interactions<sup>15,16</sup> and the internal heavy-atom effects,<sup>14</sup> and also it is interesting to know that such intersystem crossings are assumed in order to account for the high  $S_\Delta$  values of the  $\pi, \pi^*$  ketone triplet state at low temperatures.<sup>37</sup>

According to Scheme 2, the apparent quenching rate constant,  $k_q^T$ , is given by

$$k_q^T = \frac{1}{9} \frac{k_{\text{diff}} k_{\text{et}}}{k_{-\text{diff}} + k_{\text{et}}} \left\{ 1 + \left( \frac{k_{\text{isc}(1)}}{k_{-\text{diff}} + k_{\text{isc}(1)}} \right) \left( 3 + \frac{5k_{\text{isc}(2)}}{k_{-\text{diff}} + k_{\text{isc}(2)} + k_{\text{isc}(3)}} \right) + \frac{5k_{\text{isc}(3)}}{k_{-\text{diff}} + k_{\text{isc}(2)} + k_{\text{isc}(3)}} \right\} \quad (6)$$

When  $k_{\text{isc}(i)}$  ( $i = 1, 2, \text{ or } 3$ ) is negligibly small compared to  $k_{-\text{diff}}$  ( $k_{-\text{diff}} \gg k_{\text{isc}(i)}$ ) in Scheme 2,  $9k_q^T/k_{\text{diff}}$ , i.e.,  $9k_q^T/k_q^S$ , is replaced by the equation,  $9k_q^T/k_q^S = k_{\text{et}}/(k_{-\text{diff}} + k_{\text{et}})$  ( $\leq 1$ ) since  $k_{\text{diff}}$  is reasonably assumed to be  $k_q^S$ . The values of  $9k_q^T/k_q^S$  calculated using the data listed in Tables 1–5 were larger than unity for pressures above 147 MPa in *n*-butane. The pressure at which the ratio becomes larger than unity shifted to a lower value in the order of *n*-pentane, *n*-hexane, and *n*-heptane, and at 0.1 MPa in MCH the ratio was 1.06, suggesting that the contribution of  $k_{\text{isc}(i)}$  to  $k_q^T$  cannot be neglected even at 0.1 MPa and increases significantly as pressure increases.

We assume here that  $k_{\text{isc}(1)} = k_{\text{isc}(3)} (=k_{\text{isc}}^{\text{en}})$  in order to estimate the rate constants for the energy transfer and the intersystem crossing between the encounter complexes, obtaining eq 7.

$$k_q^T = \frac{1}{9} \frac{k_{\text{diff}} k_{\text{et}}}{k_{-\text{diff}} + k_{\text{et}}} \left( 1 + \frac{8k_{\text{isc}}^{\text{en}}}{k_{-\text{diff}} + k_{\text{isc}}^{\text{en}}} \right) \quad (7)$$

The unimolecular rate constant,  $k_{-\text{diff}}$ , in eq 7 is expected to be strongly dependent on pressure. Exothermic triplet–triplet energy transfer from the benzophenone triplet to naphthalene occurs with a mechanism similar to Scheme 1 in which only one encounter complex with triplet spin multiplicity is involved. From the analysis of the dependence of the rate constant for the energy transfer on the pressure-induced solvent viscosity, it was found that the bimolecular rate constant for  $k_{\text{et}}$  defined by eq 8,  $k_{\text{bim}}$ , is approximately independent of pressure.<sup>43</sup>

$$k_{\text{bim}} = (k_{\text{diff}} k_{\text{et}})/k_{-\text{diff}} \quad (8)$$

When this is applied to the quenching by oxygen, eq 7 is replaced by

$$k_q^T = \frac{1}{9} \frac{k_{\text{diff}} k_{\text{bim}}}{k_{\text{diff}} + k_{\text{bim}}} \left( 1 + \frac{8\gamma}{k_{\text{diff}} + \gamma} \right) \quad (9)$$

where  $\gamma (=k_{\text{diff}} k_{\text{isc}}^{\text{en}}/k_{-\text{diff}})$ , defined by analogy to  $k_{\text{bim}}$ , is the bimolecular rate constant for  $k_{\text{isc}}^{\text{en}}$ . If  $k_{\text{bim}}$  and  $\gamma$  are independent of pressure, eq 9 predicts that  $k_q^T/k_q^S$  can be expressed as a function of  $k_q^S$  alone, being independent of solvent and pressure. In fact, as seen in Figure 4, the plot of  $k_q^T/k_q^S$  against  $k_q^S$  indicates that it is described approximately by eq 9 in the solvents examined in this work at pressures up to 400 MPa. The values of  $k_{\text{bim}}$  and  $\gamma$  were evaluated by the curve-fitting to eq 9 using the method of nonlinear least-squares. The results are summarized in Table 6. It can be seen in Table 6 that the values of  $k_{\text{bim}}$  and  $\gamma$  are almost independent of solvent. The mean values of  $k_{\text{bim}}$  and  $\gamma$  evaluated by the curve-fitting to eq 8 using the data in five solvents (solid line in Figure 4) were  $(5.4 \pm 0.3) \times 10^{10}$  and  $(0.17 \pm 0.01) \times 10^{10} \text{ M}^{-1} \text{ s}^{-1}$ , respectively; the contribution of  $\gamma$  to  $k_q^T/k_q^S$  increases monotonically with increasing pressure (see eq 9), for example, from 0.32 at 0.1 MPa to 0.71 at 400 MPa in MCH. The results mentioned above that  $\Delta V_q^{\ddagger}$  is smaller than  $\Delta V_q^{S\ddagger}$ , and also that the plots of  $\ln k_q^T$  against  $\ln \eta$  are nonlinear may be understood in terms of the contributions of  $k_{\text{bim}}$  and  $\gamma$  to  $k_q^T$  relatively increased by a decrease in  $k_{\text{diff}} (=k_q^S)$  with increasing pressure (eq 9).

There is no available information about  $k_{\text{bim}}$  and  $\gamma$  to compare in the case of the quenching by oxygen. For energy transfers from the triplet states of benzophenone ( ${}^3n\pi^*$ ) and triphenylene ( ${}^3\pi\pi^*$ ) to naphthalene,  $k_{\text{bim}}$  was reported to be about  $1.3 \times 10^{10} \text{ M}^{-1} \text{ s}^{-1}$ , whereas it is  $3.9 \times 10^{10} \text{ M}^{-1} \text{ s}^{-1}$  for fluorescence quenching of triphenylene by benzophenone in *n*-hexane.<sup>43</sup> The value of  $k_{\text{bim}}$  ( $5.4 \times 10^{10} \text{ M}^{-1} \text{ s}^{-1}$ ) is close to that of the latter case via the encounter that has the same spin multiplicity of singlet as the present system.

Finally, the pressure independence of  $k_{\text{bim}}$  is also evident from the present study, but the reason for this is still missing. The observed rate constant in the preequilibrium limit,  $k_q^T$ , is given by  $k_{\text{bim}}/9 (k_{-\text{diff}} \gg 8k_{\text{isc}}^{\text{en}}, k_{\text{et}}$  in eq 7). It was proposed on the basis of thermodynamic considerations that the equilibrium constant,  $K (=k_{\text{diff}}/k_{-\text{diff}})$ , is approximately equal to the inverse of the molarity of the solvent,  $[S]$ .<sup>44</sup> Accordingly, since the values of  $[S]$  vary in the range 6.8–10.0 M at 0.1 MPa and 25 °C, the values of  $k_{\text{et}}$  and  $k_{\text{isc}}^{\text{en}}$  are calculated to be in the range of  $(3.7\text{--}5.5) \times 10^{11} \text{ s}^{-1}$  and  $(1.0\text{--}2.0) \times 10^{10} \text{ s}^{-1}$ , respectively. Furthermore, the volume change for the encounter complex formation,  $\Delta V$ , which is given by the equation,  $\Delta V = -RT(\partial \ln K/\partial P)_T - RT\kappa$ , where  $\kappa$  is the isothermal compressibility of the solvent, is calculated to be zero since  $\kappa = -(1/[S])(\partial[S]/\partial P)_T$ . From eq 8, one can obtain the relation,  $\Delta V_{\text{bim}}^{\ddagger} = \Delta V + \Delta V_{\text{et}}^{\ddagger}$  in which  $\Delta V = 0$  and  $\Delta V_{\text{bim}}^{\ddagger} \approx 0$ . Thus,  $\Delta V_{\text{et}}^{\ddagger} = 0$ . However, the hard-sphere theory, which has been applied successfully to many systems such as complex formation between donor and acceptor in liquid solution,<sup>45</sup> leads to different values for the volume change. According to this theory,  $\Delta V$  is evaluated to be negative (ca.  $-9$  to  $-15 \text{ cm}^3/\text{mol}$  depending on solvent<sup>46</sup>), yielding that  $\Delta V_{\text{et}}^{\ddagger} = 9\text{--}15 \text{ cm}^3/\text{mol}$ . Unfortunately however, there is no evidence that would allow further discussion about  $\Delta V_{\text{et}}^{\ddagger}$  at the present stage.

## Conclusion

The mechanism for the quenching by oxygen of the  $T_1$  state of ACA in *n*-butane, *n*-pentane, *n*-hexane, *n*-heptane, and MCH

at pressures up to 400 MPa has been investigated. It has been shown that the yields of T<sub>1</sub> state are approximately unity. The results, together with the findings that the yields for singlet oxygen formed by the quenching of the T<sub>1</sub> state are unity, have revealed that the quenching of the T<sub>1</sub> state does not involve a decay channel via the encounter complex with the spin multiplicity of triplet in all the experimental conditions examined. The ratio,  $k_q^T/k_q^S$ , where  $k_q^S$  is the diffusion-controlled quenching rate constant by oxygen of the S<sub>1</sub> state of DMEA, is about 1/9 in MCH but less than 1/9 in the other solvents at 0.1 MPa and 25 °C, and the ratio has been found to increase to over 1/9 with increasing pressure in all the solvents examined. These results have been explained by Scheme 2, which takes into account the intersystem crossing between the encounter complexes with different spin multiplicities.

**Acknowledgment.** This work was partly supported by a Grant-in-Aid for Scientific Research from the Ministry of Education of Japan 06640651 to M.O.

### References and Notes

- (1) Birks, J. B. *Photophysics of Aromatic Molecules*; Wiley-Interscience: New York, 1970; p 518.
- (2) Saltiel, J.; Atwater, B. W. *Advances in Photochemistry*; Wiley-Interscience: New York, 1987; Vol. 14, p 1.
- (3) Ware, W. R. *J. Phys. Chem.* **1962**, *66*, 455.
- (4) Yasuda, H.; Scully, A. D.; Hirayama, S.; Okamoto, M.; Tanaka, F. *J. Am. Chem. Soc.* **1990**, *112*, 6847.
- (5) Hirayama, S.; Yasuda, H.; Scully, A. D.; Okamoto, M. *J. Phys. Chem.* **1994**, *98*, 4609.
- (6) Gijzeman, O. L. J.; Kaufman, F.; Porter, G. *J. Chem. Soc., Faraday Trans. 2* **1973**, *69*, 708.
- (7) Wilkinson, F.; McGravey, D. J.; Olea, A. F. *J. Am. Chem. Soc.* **1993**, *115*, 12151.
- (8) Olea, A. F.; Wilkinson, F. *J. Phys. Chem.* **1995**, *99*, 4518.
- (9) Redmond, R. W.; Braslavsky, S. E. *Chem. Phys. Lett.* **1988**, *148*, 523.
- (10) Darmanyan, A. P.; Foote, C. S. *J. Phys. Chem.* **1993**, *97*, 5032.
- (11) McGravey, D. J.; Szekeres, P. G.; Wilkinson, F. *Chem. Phys. Lett.* **1992**, *199*, 314.
- (12) Wilkinson, F.; McGravey, D. J.; Olea, A. F. *J. Phys. Chem.* **1994**, *98*, 3762.
- (13) Wilkinson, F.; Abdel-Shafi, A. A. *J. Phys. Chem. A* **1997**, *101*, 5509.
- (14) Darmanyan, A. P.; Foote, C. S. *J. Phys. Chem.* **1992**, *96*, 3728.
- (15) Garner, A.; Wilkinson, F. *Chem. Phys. Lett.* **1977**, *45*, 432.
- (16) Grewer, C.; Brauer, H.-D. *J. Phys. Chem.* **1994**, *98*, 4230.
- (17) Mitchell, D. J.; Schuster, G. B.; Drickamer, H. G. *J. Am. Chem. Soc.* **1977**, *99*, 1145.
- (18) Bondi, A. *J. Phys. Chem.* **1964**, *68*, 441.
- (19) Okamoto, M.; Teranishi, H. *J. Phys. Chem.* **1984**, *88*, 5644.
- (20) Okamoto, M.; Teranishi, H. *J. Am. Chem. Soc.* **1986**, *108*, 6378.
- (21) Murrov, S. L. *Handbook of Photochemistry*; Marcel Dekker: New York, 1973.
- (22) IUPAC Analytical Chemistry Division, Commission on Solubility Data *Oxygen and Ozone*; Solubility Data Series; Battino, R., Ed.; Pergamon: Oxford, 1981; Vol. 7.
- (23) Kiran, E.; Sen, Y. L. *Int. J. Thermophys.* **1992**, *13*, 411.
- (24) Diller, D. E.; Van Poolen, L. *J. Int. J. Thermophys.* **1985**, *6*, 43.
- (25) Babb, S. E., Jr.; Scott, G. J. *J. Chem. Phys.* **1964**, *40*, 3666.
- (26) Bridgman, P. W. *Proc. Am. Acad. Arts. Sci.* **1926**, *61*, 57.
- (27) Brazier, D. W.; Freeman, G. R. *Can. J. Chem.* **1969**, *47*, 893.
- (28) Oliveira, C. M. B. P.; Wakeham, W. A. *Int. J. Thermophys.* **1992**, *13*, 773.
- (29) Collings, A. F.; McLaughlin, E. *Trans. Faraday. Soc.* **1971**, *67*, 340.
- (30) Dymond, J. H.; Young, K. J.; Isdale, J. D. *Int. J. Thermophys.* **1980**, *1*, 345.
- (31) Assael, M. J.; Oliveria, C. P.; Papadaki, M.; Wakeham, W. A. *Int. J. Thermophys.* **1992**, *13*, 593.
- (32) Jonas, J.; Hasha, D.; Huang, S. G. *J. Chem. Phys.* **1979**, *71*, 15.
- (33) Okamoto, M.; Tanaka, F. *J. Phys. Chem.* **1993**, *97*, 177.
- (34) Okamoto, M.; Tanaka, F.; Teranishi, H. *J. Phys. Chem.* **1990**, *94*, 669.
- (35) Okamoto, M. *J. Phys. Chem.* **1992**, *96*, 245.
- (36) Hirayama, S.; Yasuda, H.; Okamoto, M.; Tanaka, F. *J. Phys. Chem.* **1991**, *95*, 2971.
- (37) Grewer, C.; Brauer, H.-D. *J. Phys. Chem.* **1993**, *97*, 5001.
- (38) Hirayama, S.; Kobayashi, T. *Chem. Phys. Lett.* **1977**, *52*, 55.
- (39) Hirayama, S. *J. Chem. Soc., Faraday Trans. 1* **1982**, *78*, 2411.
- (40) Tanaka, F. Unpublished results.
- (41) Schmidt, R.; Sekel, K.; Brauer, H.-D. *Ber. Bunsen-Ges. Phys. Chem.* **1990**, *94*, 1100.
- (42) Gorman, A. A.; Hamblett, I.; Lambert, A. L.; Prescott, A. L.; Rodgers, A. J.; Spence, H. M. *J. Am. Chem. Soc.* **1987**, *109*, 3091.
- (43) Okamoto, M. *J. Phys. Chem. A* **1998**, *102*, 4751.
- (44) Saltiel, J.; Shannon, P. T.; Zafiriou, O. C.; Uriarte, K. *J. Am. Chem. Soc.* **1980**, *102*, 6799.
- (45) Yoshimura, Y.; Nakahara, M. *J. Chem. Phys.* **1984**, *81*, 4080.
- (46) The following values were used in the calculation of  $\Delta V$ : hard sphere radius, 0.173 (oxygen) and 0.356 nm (ACA); RT $\kappa$ , 4.5 (*n*-butane), 3.7 (*n*-pentane), 3.1 (*n*-hexane), and 2.2 cm<sup>3</sup>/mol (MCH).